Analysis of Temperature Resistance of Pressurized Cylindrical Fuel Tanks

Assoc. Prof. PhD. Eng. **Mihai ŢĂLU**[1], Assoc. Prof. PhD. Eng. **Ștefan ŢĂLU**[2,*]

[1] University of Craiova, Faculty of Mechanics, Department of Applied Mechanics and Civil Engineering, Calea București Street, no. 107, 200512 Craiova, Dolj county, Romania. E-mail: mihai_talu@yahoo.com

[2] Technical University of Cluj-Napoca, The Directorate of Research, Development and Innovation Management (DMCDI), Constantin Daicoviciu Street, no. 15, Cluj-Napoca, 400020, Cluj county, Romania. Corresponding author* e-mail: stefan_ta@yahoo.com

Abstract: *In this study, an approach based on Finite Element Modeling (FEM) was applied to analyze the performances of three different pressurized cylindrical fuel tanks with the same lateral cover, but with various head covers geometries. A specific mechanical and thermal model based on FEM was developed. A particular analysis of temperature resistance was carried out, to define specific key performance indicators and to determine the advantageous form of tank with the minimum stress state and linear deformation.*

Keywords: *Automotive industry, corrosion, industrial engineering design, optimization methods, pressurized cylindrical fuel tank, temperature resistance*

1. Introduction

In the past decades, the fuel tanks market trend is based on key strategic business plans that promote the competitive paths in the emerging automotive field and in promoting innovative ideas to improve vehicle's performance [1-6].
The challenge for the engineers and research specialists is to formulate a sustainable strategy based on a rigorous research and analysis that promotes the development computer aided engineering process of modern fuel tanks, especially over the medium to long term, within the constraints due to the economic and financial crisis [7-12].
Cylindrical and conformable shaped storage tanks, made from aluminum alloys or various types of steel, are used in the automotive industry for safely storing fuel: compressed natural gas (CNG) or liquefied petroleum gas (LPG) [11-14].
In computer aided engineering design and construction of the fuel tanks: specific structure variables [13-15], shape design variables [16, 17], design constraints [18, 19], software tools [20-25], and design decision variables [26-28] are used to validate the optimal computational geometric models [29-36].
The homologation tests of systems and components for LPG and CNG alternative fuelling of cars according to ECE Regulation No. 67.01, ECE Regulation No. 110 and standards ISO 15500 are [37, 38]:
a) Hydrostatic pressure tests: • pressure vessel tests; • destructive tests up to a static pressure of 300 MPa; • residual strength tests; • metal as well as composite hydraulic member tests; • hydraulic hose tests.
b) Hydrodynamic pressure tests: • pulsed pressure tests; • cyclic stress tests; • cyclic stress tests of hoses.
c) Temperature and humidity tests: • tests of devices at extreme temperatures (-70 to 180 ^{0}C) and relative humidity from 10 % to 95 % up to dimensions 1000 x 1000 x 2500 mm.

2. Design methodology

In our study the test of temperature resistance, one of the special safety tests of cylindrical pressurized fuel tanks carried out at the homologation stage, was performed.
The parameterized modeling of the cylindrical pressurized fuel tank (sectioned to *½ , ¼ or* $^1/_8$ of the initial model, as a consequence of the tank constructive symmetry) was done in the AutoCAD

Autodesk 2017 software [39], which was imported to SolidWorks 2017 software [40] for analysis with the: Static, Thermal and Design Study modules.
The 3D parameterized models were thermally loaded at the specified stress state to determine the maximum work temperature T_{max} and the explosion temperature T_r, at the initial and final time of exploitation of the fuel tank.
The design data used in this analysis are:

- the lateral cover with: diameter D = 250 mm and length L = 700 mm;
- the construction material of the sheet metal: steel AISI 4340;
- the maximum static hydraulic pressure: p_{max} = 30 bar;
- the working temperature between the limits: T = -30 ^{0}C to T = 60 ^{0}C;
- the exploitation period of tank: n_a = 20 years;
- the corrosion rate of the material: v_c = 0.1 mm /year.

The temperature resistance means: the maximum temperature at which the resulting stress Von Mises is equal to the admissible stress traction of material $\sigma_{rez} = \sigma_a$ and the explosion temperature is the temperature at which the Von Mises stress attain the breaking stress of the material $\sigma_{rez} = \sigma_r$.

2.1 The study at temperature resistance of the cylindrical lateral cover

The parameterized model used in calculus is a section of ¼ from the initial lateral cover of tank, taking into consideration the axial symmetry (figure 1) and the specified surfaces to which the constraints and restrictions are applied (figure 2) [8].

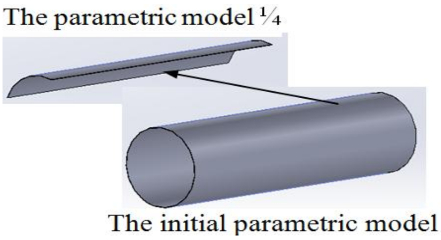

Fig. 1. The parametric model of lateral covers

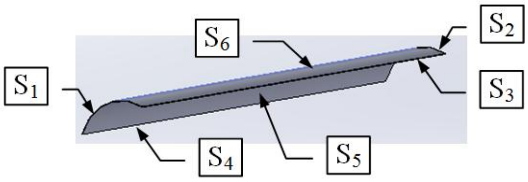

Fig. 2. The ¼ section of lateral head covers where is made the marking of the exterior surfaces

Applying the optimization procedure, a laminate sheet of AISI 4340 steel with a thickness of $s = 4^{+0.25}_{-0.6}$ mm is chosen for FEM analyses.
According to Fig. 2, to calculate the temperatures: T_{max} and T_r, the following algorithm was applied:

- the maximum pressure p_{max} = 3 N/mm^2 on inner surface S_5;
- two opposite and equal traction forces, F = 36800 N applied on surfaces: S_1 and S_2, due to the action of pressure on the inner surface of head covers;
- the high temperature on surface S_6, over T > 60 ^{0}C in order to achieve the admissible value of stress at traction equal with σ_a = 710 N/mm^2 (necessary to calculate the work maximum temperature T_{max}); and the high temperature in order to achieve the breaking stress of material with σ_r = 1100 N/mm^2 (necessary to calculate the explosion temperature T_r);
- the construction material of the lateral cover: steel AISI 4340.

The following numerical results for lateral cover were obtained:
a) for n_a = 0 years: T_{max} = 302.65 ^{0}C with the corresponding stress distribution (as shown in figure 3a); and T_r = 474.2 ^{0}C, with the corresponding stress distribution (as shown in figure 3b).
b) for n_a = 20 years: T_{max} = 182.85 ^{0}C, with the corresponding stress distribution (as shown in figure 3c); and T_r = 336.87 ^{0}C, with the corresponding stress distribution (as shown in figure 3d).

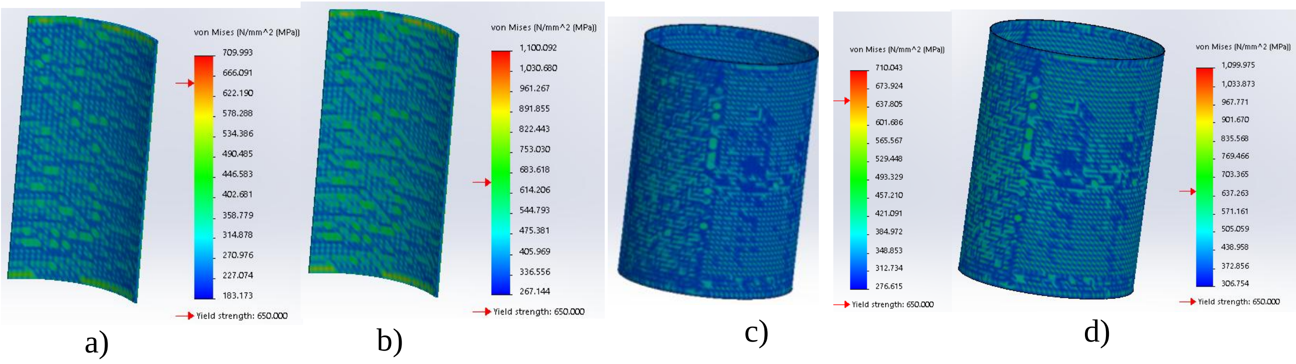

Fig. 3. The graphs of Von Mises stress distribution at: a) the temperature T_{max} and n_a = 0 years; b) the explosion temperature T_r and n_a = 0 years; c) the temperature T_{max} and n_a = 20 years; d) the explosion temperature T_r and n_a = 20 years

2.2 The study at temperature resistance of the cylindrical pressurized tank with torospheric head covers

The parameterized model of tank (as shown in figure 4) and the sketch of torospheric head cover (as shown in figure 5) are given bellow:

Fig. 4. The parametric model of tank with torospheric head covers

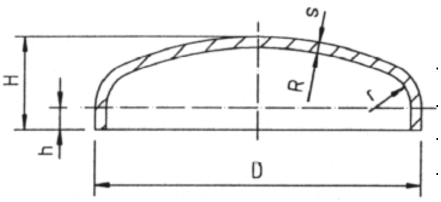

$$r = 0.1 \cdot D$$
$$R = D$$
$$h \cong 3.5s$$
$$H = 0.2D + s + h$$

Fig. 5. The sketch of torospheric head cover

After design optimization a laminate sheet of AISI 4340 steel with a thickness of $s = 5.5^{+0.25}_{-0.6}$ mm it was chosen for the manufacturing process (as shown in figure 5). Next dimensions were obtained for the head cover: R = 250 mm, r = 25 mm, h = 20 mm and H = 75.5 mm.
The following numerical results were obtained for Von Mises stress distribution at n_a = 0 years: T_{max} = 232.22 ^{0}C with the corresponding stress distribution (as shown in figures 6a and 6b); and T_r = 363.39 ^{0}C, with the corresponding stress distribution (as shown in figures 6c and 6d).
The graphs of Von Mises stress distribution were shown on the sectioned model at $^1/_8$ in figures 6a and 6c and in figures 6b and 6d for the entire model.

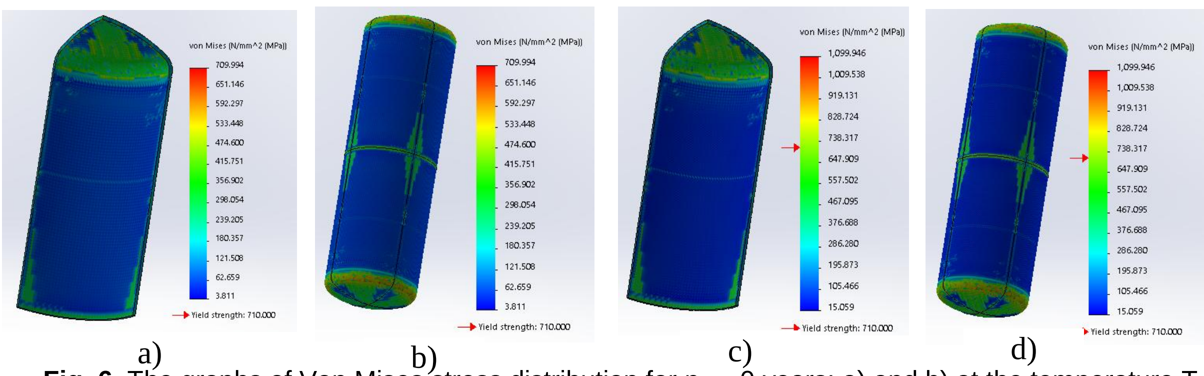

Fig. 6. The graphs of Von Mises stress distribution for n_a = 0 years: a) and b) at the temperature T_{max}; c) and d) at the explosion temperature T_r

The following numerical results were obtained for Von Mises stress distribution at n_a = 20 years: T_{max} = 156.18 ^{0}C with the corresponding stress distribution (as shown in figures 7a and 7b); and T_r = 283.3 ^{0}C, with the corresponding stress distribution (as shown in figures 7c and 7d).

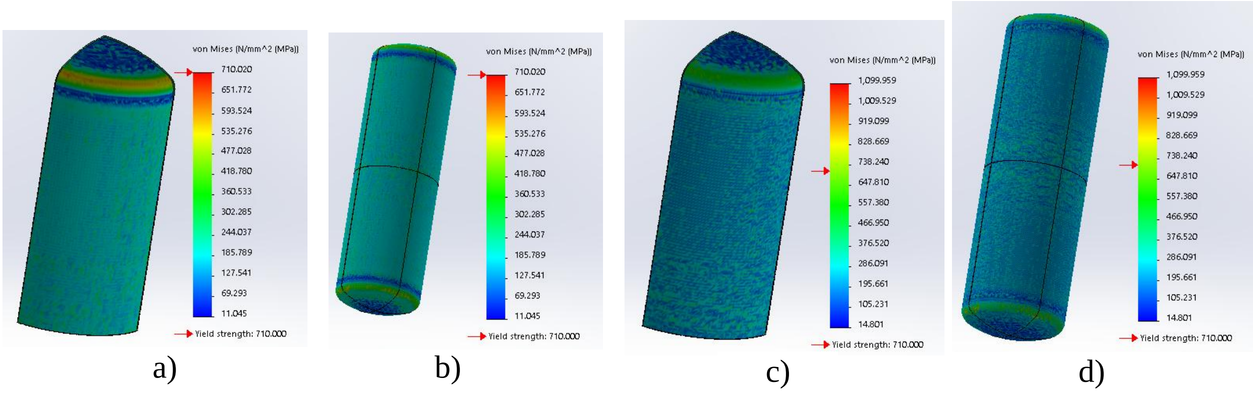

Fig. 7. The graphs of Von Mises stress distribution for n_a = 20 years: a) and b) at the temperature T_{max}; c) and d) at the explosion temperature T_r

2.3 The study at temperature resistance of the cylindrical pressurized tank with ellipsoidal head covers

The parameterized model of tank (as shown in figure 8) and the sketch of ellipsoidal head cover (as shown in figure 9) are given bellow:

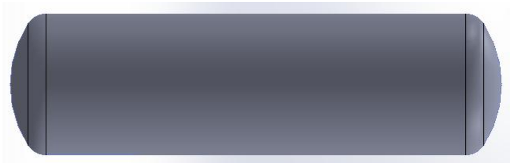

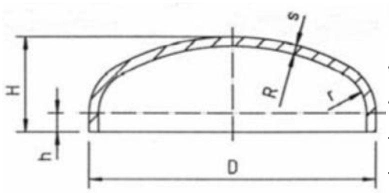

– $r = 0.154 \cdot D$
– $R = 0.8 \cdot D$
– $h \cong 3.5s$
– $H = 0.26 \cdot D + s + h$

Fig. 8. The parametric model of tank with ellipsoidal head covers

Fig. 9. The sketch of ellipsoidal head cover according the standard DIN 28013

After design optimization a laminate sheet of AISI 4340 steel with a thickness of s = $4.5^{+0.25}_{-0.6}$ mm it was chosen for the manufacturing process (as shown in figure 9). Next dimensions were obtained for the ellipsoidal cover: R = 200 mm, r = 38.5 mm, h = 16 mm and H = 85.5 mm.

The following numerical results were obtained for Von Mises stress distribution at n_a = 0 years: T_{max} = 271.55 ^{0}C, with the corresponding stress distribution (as shown in figures 10a and 10b); and T_r = 407.15 ^{0}C, with the corresponding stress distribution (as shown in figures 10c and 10d).

The graphs of Von Mises stress distribution were shown on the sectioned model at $^1/_8$ in figures 10a and 10c and in figures 10b and 10d for the entire model.

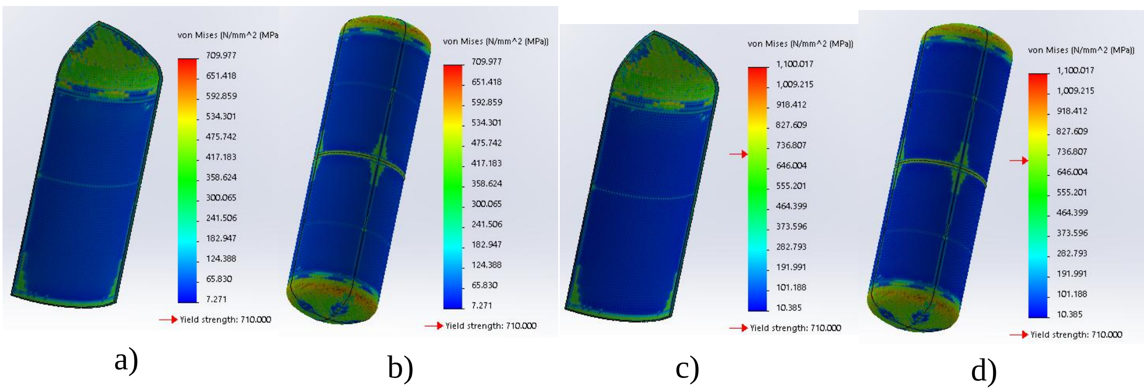

Fig. 10. The graphs of Von Mises stress distribution for n_a = 0 years: a) and b) at the temperature T_{max}; c) and d) at the explosion temperature T_r

The following numerical results were obtained for Von Mises stress distribution at n_a = 20 years: T_{max} = 155.07 ^{0}C, with the corresponding stress distribution (as shown in figures 11a and 11b); T_r = 280.85 ^{0}C, with the corresponding stress distribution (as shown in figures 11c and 11d).

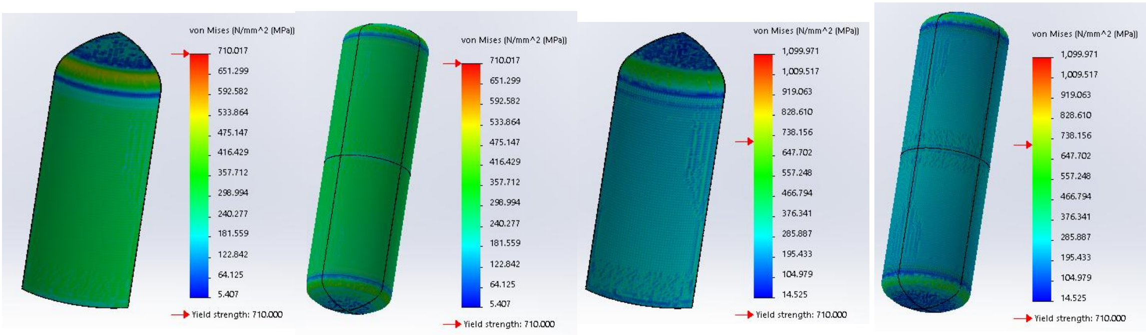

a) b) c) d)

Fig. 11. The graphs of Von Mises stress distribution for n_a = 20 years: a) and b) at the temperature T_{max}; c) and d) at the explosion temperature T_r

2.4 The study at temperature resistance of the cylindrical pressurized tank low pressure head covers

The parameterized model of tank (as shown in figure 12) and the sketch of the low pressure head cover (as shown in figure 13) are given bellow:

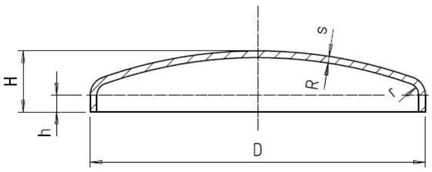

– $r = [15..40]\text{mm}$
– $h = [20..25]\text{mm}$
– $H = 0.13 \cdot D + s + h$

Fig. 12. The parametric model of tank with low pressure head covers

Fig. 13. The sketch of the low pressure head cover

After design optimization a laminate sheet of AISI 4340 steel with a thickness of $s = 6.5^{+0.25}_{-0.6}$ mm it was chosen for the manufacturing process (as shown in Figure 13). Next dimensions were obtained for the low pressure head cover: h = 22 mm, r = 15 mm and H = 61 mm.
The following numerical results were obtained for Von Mises stress distribution at n_a = 0 years: T_{max} = 222.25 ^{0}C, with the corresponding stress distribution (as shown in figures 14a and 14b); and T_r = 360.94 ^{0}C, with the corresponding stress distribution (as shown in figures 14c and 14d).
The graphs of Von Mises stress distribution were shown on the sectioned model at $^1/_8$ in figures 14a and 14c and in figures 14b and 14d for the entire model.

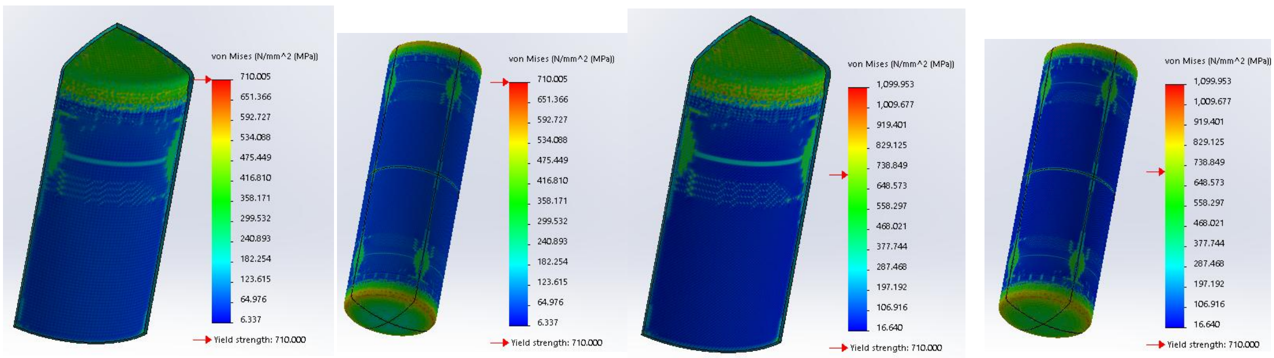

a) b) c) d)

Fig. 14. The graphs of Von Mises stress distribution for n_a = 0 years: a) and b) at the temperature T_{max}; c) and d) at the explosion temperature T_r

The following numerical results were obtained for Von Mises stress distribution at n_a = 20 years: T_{max} = 150.2 ^{0}C, with the corresponding stress distribution (as shown in figures 15a and 15b); T_r = 275.55 ^{0}C, with the corresponding stress distribution (as shown in figures 15c and 15d).

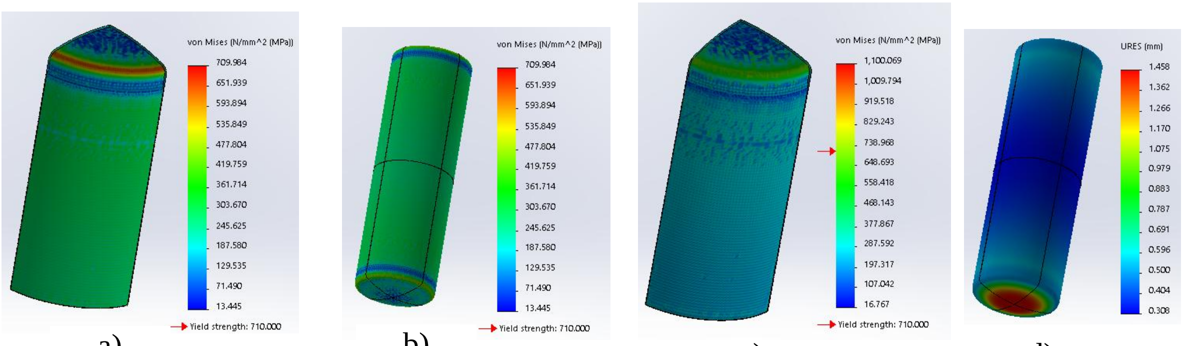

Fig. 15. The graphs of Von Mises stress distribution for n_a = 20 years: a) and b) at the temperature T_{max}; c) and d) at the explosion temperature T_r

The linear deformation corresponding to the extreme temperatures were also computed. The numerical values of state of stress and linear resultant deformation of the tanks are given in Table 1.

Table 1: The Von Mises stress and deformation of tanks at temperatures T_{max} and T_r

No.	The type of cylindrical tank	n_a [years]	T_{max} [^{0}C]	u_{max} [mm]	T_r [^{0}C]	u_r [mm]
			σ_a = 710 MPa		σ_r = 1100 MPa	
1	Tank with torosferic head covers	0	232.22	0.541	363.39	0.744
		20	156.18	0.796	283.30	0.932
2	Tank with ellipsoidal head covers	0	271.55	0.55	407.15	0.783
		20	155.07	0.782	280.85	1.005
3	Tank with low pressure head covers	0	225.25	0.713	360.94	0.912
		20	150.20	1.192	275.55	1.458

The graphical representations of $T_{max}(n_{tank})$ and $T_r(n_{tank})$ depending on the number’s tank as specified in Table 1, computed for the initial and the final time of exploitation are shown in figures 16 and 17.

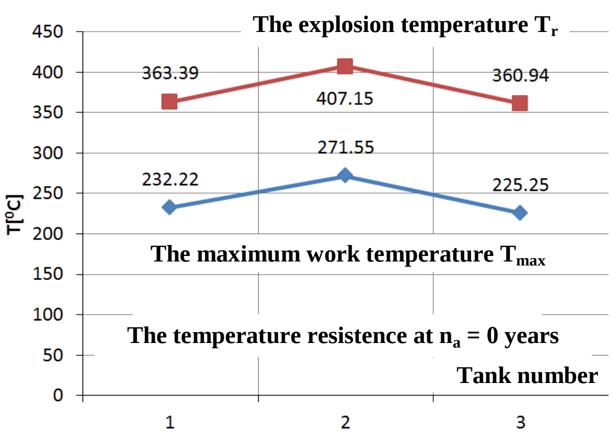

Fig. 16. The graphs of $T_r(n_{tank})$ and $T_{max}(n_{tank})$ at n_a = 0 years

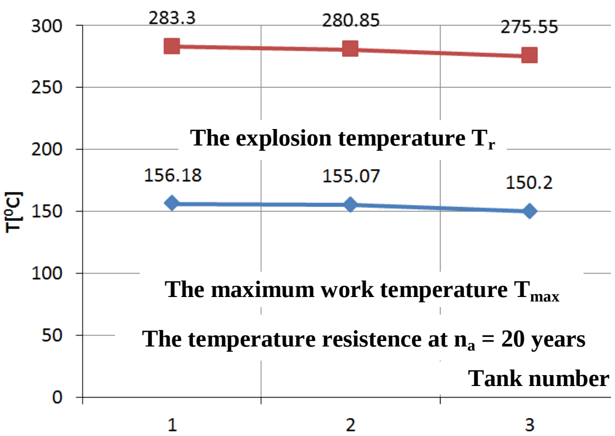

Fig. 17. The graphs of $T_r(n_{tank})$ and $T_{max}(n_{tank})$ at n_a = 20 years

The graphical representations of $T_{max}(n_{tank})$ and $T_r(n_{tank})$ depending on the number’s tank as specified in Table 1, computed for the initial and the final time of exploitation (arranged on the same graph) are shown in figures 18 and 19.

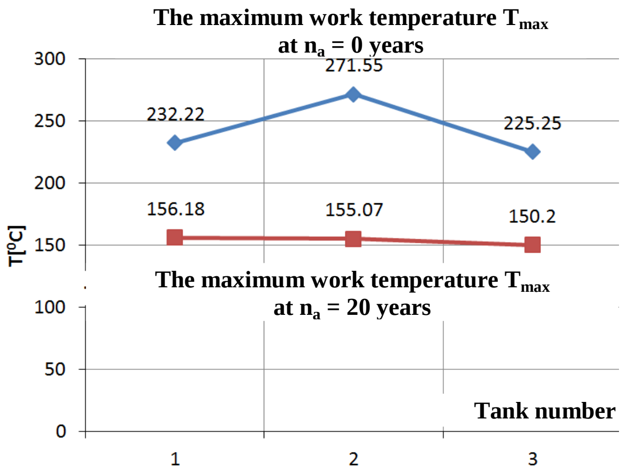

Fig. 18. The graphs of $T_{max}(n_{tank})$ at n_a = 0 and 20 years

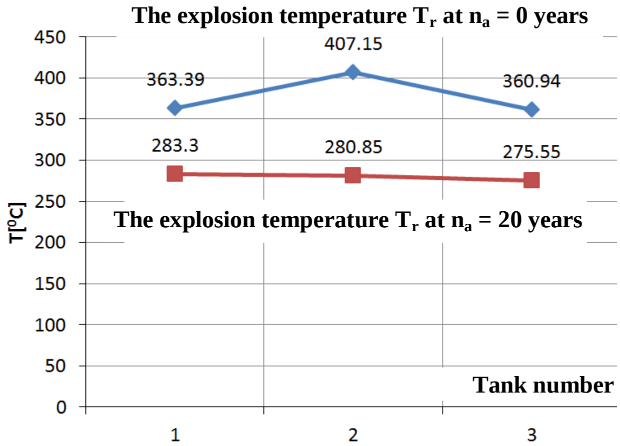

Fig. 19. The graphs of $T_r(n_{tank})$ at n_a = 0 and 20 years

The graphical representations of $T_{max}(n_a, n_{tank})$ and $T_r(n_a, n_{tank})$ are shown in figures 20 and 21.

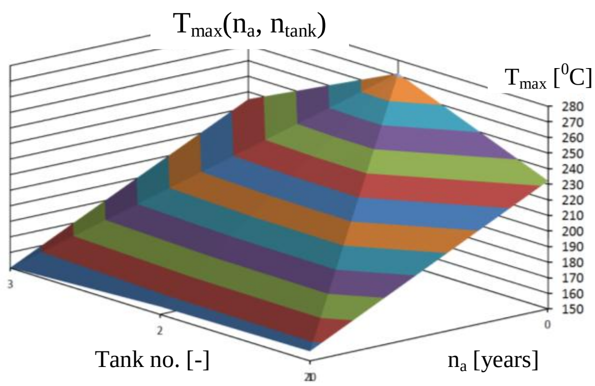

Fig. 20. The 3D graph of $T_{max}(n_a, n_{tank})$

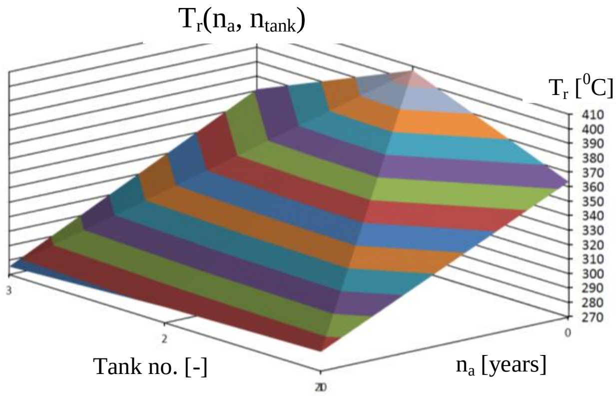

Fig. 21. The 3D graph of $T_r(n_a, n_{tank})$

The graphical representations of $u_{max}(n_{tank})$ and $u_r(n_{tank})$ depending on the number's tank as specified in Table 1, computed for the initial and the final time of exploitation are shown in figures 22 and 23.

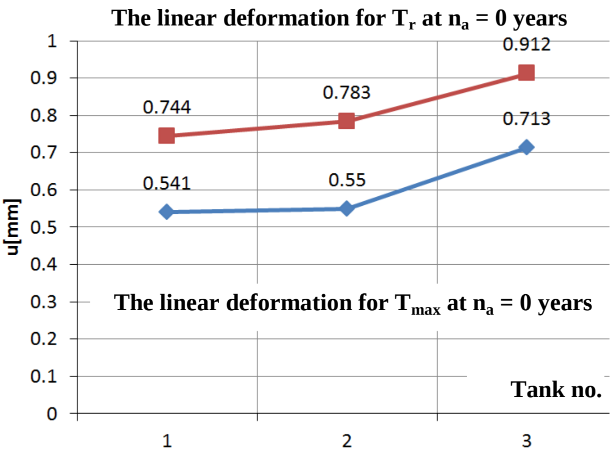

Fig. 22. The graphs of $u(n_a)$ for T_r and T_{max} at n_a = 0 year

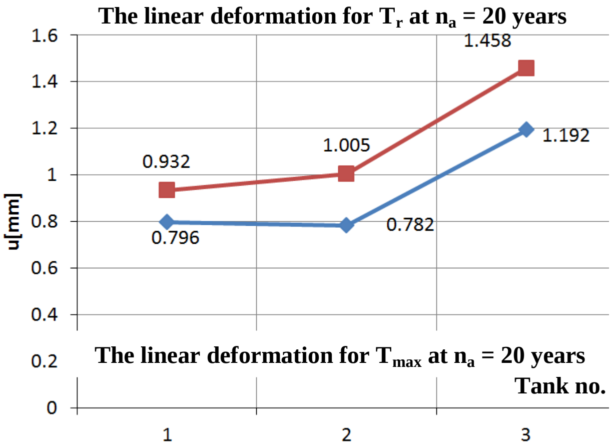

Fig. 23. The graphs of $u(n_a)$ for T_r and T_{max} at n_a = 20 years

The graphical representations of $u_{max}(n_{tank})$ and $u_r(n_{tank})$ depending on the number's tank as specified in Table 1, computed for the initial and the final time of exploitation (and arranged on the same graph for T_{max} and T_r) are shown in figures 24 and 25.

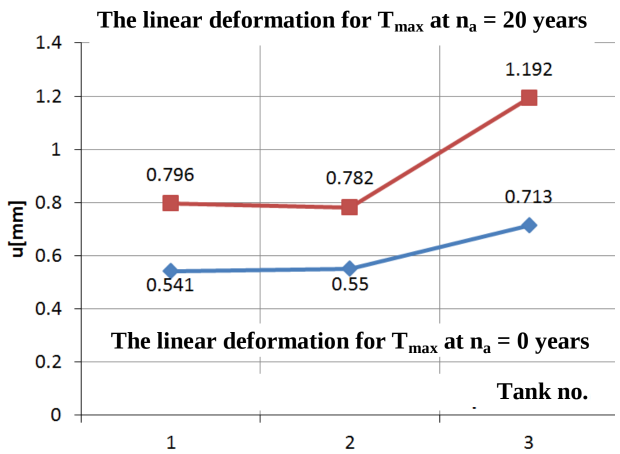

Fig. 24. The graphs of $u(n_a, n_{tank})$ for T_{max}

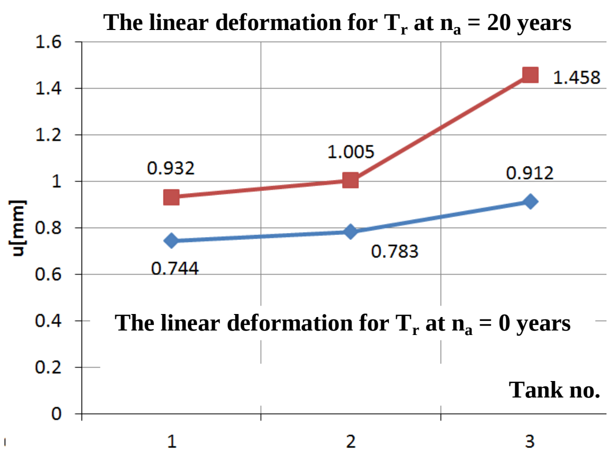

Fig. 25. The graphs of $u(n_a, n_{tank})$ for T_r

The graphical representations of $u_{max}(n_a, n_{tank})$ and $u_r(n_a, n_{tank})$ are shown in figures 26 and 27.

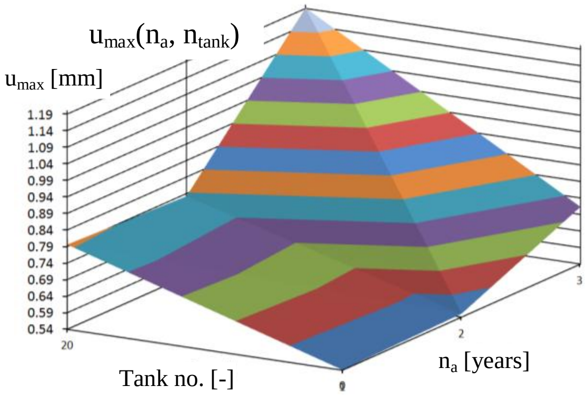

Fig. 26. The 3D graph of $u_{max}(n_a, n_{tank})$

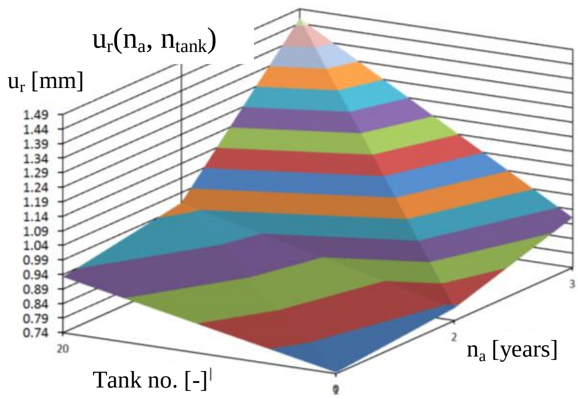

Fig. 27. The 3D graph of $u_r(n_a, n_{tank})$

3. Discussion

The tank with ellipsoidal head covers (at n_a = 0 years) has the highest work temperature T_{max} = 271.55 ^{0}C and the highest explosion temperature T_r = 407.15 ^{0}C, while the tank with low pressure head covers has the lowest work temperature T_{max} = 225.25 ^{0}C and the lowest explosion temperature T_r = 360.94 ^{0}C, (as shown in figure 16).
The tank with torospheric head covers (at n_a = 20 years) has the highest working temperature T_{max} = 156.18 ^{0}C and explosion temperature T_r = 283.3 ^{0}C; while the tank with low pressure head covers has the lowest work temperature T_{max} = 150.2 ^{0}C and explosion temperature T_r = 275.55 ^{0}C, (as shown in figure 17).
The tank with low pressure head covers (at n_a = 0 years, for T_{max} and T_r) has the maximum linear deformation u_{max} = 0.713 mm and u_r = 0.912 mm; while the tank with torospheric head covers has the lowest deformation u_{max} = 0.541 mm and u_r = 0.744 mm, (as shown in figure 22).
The tank with low pressure head covers (at n_a = 20 years, for T_{max} and T_r) has the maximum linear deformation u_{max} = 1.192 mm and u_r = 1.458 mm; while the tank with ellipsoidal head covers has the lowest deformation u_{max} = 0.782 mm and u_r = 1.005 mm.

4. Conclusions

In this study, were analyzed the performances of three different pressurized cylindrical fuel tanks with the same lateral cover, but with various head covers geometries. It was found that the

temperature resistance, the Von Mises stress and deformation are influenced by the tank geometry.
The highest temperature resistance (at n_a = 0 years) was found for the tank with ellipsoidal head covers, while the lowest temperature resistance was found for the tank with low pressure head covers.
The highest temperature resistance (at n_a = 20 years) was found for the tank with torospheric head covers, while the lowest temperature resistance was found for the tank with low pressure head covers.
The lowest linear deformation was found for the tank with torospheric head covers, while the maximum deformation was found for the tank with low pressure head covers.

Financial disclosure: Neither author has a financial or proprietary interest in any material or method mentioned.
Competing interests: The authors declare that they have no significant competing financial, professional or personal interests that might have influenced the performance or presentation of the work described in this manuscript.

References

[1] Ghiţă, C. Mirela, Anton C. Micu, Mihai Ţălu, Ştefan Ţălu and Ema I. Adam. "Computer-Aided Design of a classical cylinder gas tank for the automotive industry." *Annals of Faculty of Engineering Hunedoara - International Journal of Engineering, Hunedoara*, *Romania*, Tome XI, Fascicule 4 (2013): 59-64.
[2] Ghiţă, C. Mirela, Anton C. Micu, Mihai Ţălu and Ştefan Ţălu. "3D modelling of a gas tank with reversed end up covers for automotive industry.", *Annals of Faculty of Engineering Hunedoara - International Journal of Engineering, Hunedoara*, *Romania*, Tome XI, Fascicule 3 (2013): 195-200.
[3] Ghiţă, C. Mirela, Anton C. Micu, Mihai Ţălu and Ştefan Ţălu. "Shape optimization of vehicle's methane gas tank." *Annals of Faculty of Engineering Hunedoara - International Journal of Engineering, Hunedoara, Romania*, Tome X, Fascicule 3 (2012): 259-266.
[4] Ghiţă, C. Mirela, Anton C. Micu, Mihai Ţălu and Ştefan Ţălu. "3D modelling of a shrink fitted concave ended cylindrical tank for automotive industry." *Acta Technica Corviniensis – Bulletin of Engineering, Hunedoara, Romania*, Tome VI, Fascicule 4 (2013): 87-92.
[5] Ghiţă, C. Mirela, Ştefan C. Ghiță, Ştefan Ţălu and Simona Rotaru, "Optimal design of cylindrical rings used for the shrinkage of vehicle tanks for compressed natural gas." *Annals of Faculty of Engineering Hunedoara - International Journal of Engineering, Hunedoara*, Tome XII, Fascicule 3 (2014): 243-250.
[6] Ghiţă, C. Mirela, Anton C. Micu, Mihai Ţălu and Ştefan Ţălu. "Shape optimization of a thoroidal methane gas tank for automotive industry." *Annals of Faculty of Engineering Hunedoara - International Journal of Engineering, Hunedoara, Romania*, Tome X, Fascicule 3 (2012): 295-297.
[7] Ţălu, Ştefan and Mihai Ţălu. "The influence of deviation from circularity on the stress of a pressurized fuel cylindrical tank." *Magazine of Hydraulics, Pneumatics, Tribology, Ecology, Sensorics, Mechatronics (HIDRAULICA)*, no. 4 (December 2017): 34-45.
[8] Bică, Marin, Mihai Ţălu and Ştefan Ţălu. "Optimal shapes of the cylindrical pressurized fuel tanks." *Magazine of Hydraulics, Pneumatics, Tribology, Ecology, Sensorics, Mechatronics (HIDRAULICA)*, no. 4 (December 2017): 6-17.
[9] Ţălu, Mihai. "The influence of the corrosion and temperature on the Von Mises stress in the lateral cover of a pressurized fuel tank." *Magazine of Hydraulics, Pneumatics, Tribology, Ecology, Sensorics, Mechatronics (HIDRAULICA)*, no. 4 (December 2017): 89-97.
[10] Vintilă, Daniela, Mihai Ţălu and Ştefan Ţălu. "The CAD analyses of a torospheric head cover of a pressurized cylindrical fuel tank after the crash test." *Magazine of Hydraulics, Pneumatics, Tribology, Ecology, Sensorics, Mechatronics (HIDRAULICA)*, no. 4 (December 2017): 57-66.
[11] Ţălu, Mihai and Ştefan Ţălu. "Design and optimization of pressurized toroidal LPG fuel tanks with variable section." *Magazine of Hydraulics, Pneumatics, Tribology, Ecology, Sensorics, Mechatronics (HIDRAULICA)*, no. 1 (March 2018): 32-41.
[12] Kișioglu, Yasin. "Burst tests and volume expansions of vehicle toroidal LPG fuel tanks." *Turkish J. Eng. Env.*, vol. 33 (2009): 117-125. DOI: 10.3906/muh-0905-2.
[13] Patel, M. Pankit and Jaypalsinh Rana. "Design & optimization of LNG-CNG cylinder for optimum weight." *IJSRD - International Journal for Scientific Research & Development*, vol. 1, issue 2 (2013): 282-286.
[14] Gopi, Remya and Beena B.R. "Finite Element Analysis OF GFRP LPG Cylinder." *IJEDR - International Journal of Engineering Development and Research*, vol. 3, issue 4 (December 2015): 642-649.

[15] Khobragade, Rashmi and Vinod Hiwase. "Design, and analysis of pressure vessel with hemispherical and flat circular end." *International Journal of Engineering Science and Computing*, vol. 7, no. 5 (2017): 12458-12469.
[16] Ţălu, Ştefan and Mihai Ţălu. "CAD generating of 3D supershapes in different coordinate systems." *Annals of Faculty of Engineering Hunedoara - International Journal of Engineering, Hunedoara, Romania*, Tome VIII, Fascicule 3 (2010): 215-219.
[17] Ţălu, Ştefan and Mihai Ţălu. "A CAD study on generating of 2D supershapes in different coordinate systems." *Annals of Faculty of Engineering Hunedoara - International Journal of Engineering, Hunedoara, Romania*, Tome VIII, Fascicule 3 (2010): 201-203.
[18] Ziółkowska, Monika and Dorota Wardzińska. "Corrosiveness of fuels during storage processes", published by IntechOpen. Accessed January 10, 2018. http://dx.doi.org/10.5772/59803.
[19] Mould, Peter, Terry Burton, Rick Daley, Shinichi Itonaga, Toshihiro Kikuchi, Sue Jokela, Michel Luciani, Matt McCosby, Doug Paul, Tetsuo Sakiyama, Gerd Schwerzel, Ray Sheffield, Greg Tarrance and Wilhelm Warnecke. "Evaluation of the corrosion durability of steel systems for automobile fuel tanks." SAE Technical Paper 2005-01-0540, 2005. Accessed January 10, 2018. https://doi.org/10.4271/2005-01-0540.
[20] Ţălu, Ştefan. *Limbajul de programare AutoLISP. Teorie şi aplicaţii. (AutoLISP programming language. Theory and applications)*. Cluj-Napoca, Risoprint Publishing house, 2001.
[21] Ţălu, Ştefan. *Reprezentări grafice asistate de calculator. (Computer assisted graphical representations).* Cluj-Napoca, Osama Publishing house, 2001.
[22] Ţălu,,Ştefan. *Grafică tehnică asistată de calculator. (Computer assisted technical graphics)*. Cluj-Napoca, Victor Melenti Publishing house, 2001.
[23] Ţălu, Ştefan. *AutoCAD 2005*. Cluj-Napoca, Risoprint Publishing house, 2005.
[24] Ţălu, Ştefan and Mihai Ţălu. *AutoCAD 2006. Proiectare tridimensională. (AutoCAD 2006. Three-dimensional designing)*. Cluj-Napoca, MEGA Publishing house, 2007.
[25] Ţălu, Ştefan. *AutoCAD 2017*. Cluj-Napoca, Napoca Star Publishing house, 2017.
[26] Țălu, Mihai. *Calculul pierderilor de presiune distribuite în conducte hidraulice. (Calculation of distributed pressure loss in hydraulic pipelines).* Craiova, Universitaria Publishing house, 2016.
[27] Țălu, Mihai. *Pierderi de presiune hidraulică în conducte tehnice cu secțiune inelară. Calcul numeric și analiză C.F.D. (Hydraulic pressure loss in technical piping with annular section. Numerical calculation and C.F.D.)*, Craiova, Universitaria Publishing house, 2016.
[28] Ţălu, Mihai. *Mecanica fluidelor. Curgeri laminare monodimensionale. (Fluid mechanics. The monodimensional laminar flow).* Craiova, Universitaria Publishing house, 2016.
[29] Ţălu, Ştefan. *Geometrie descriptivă. (Descriptive geometry)*, Cluj-Napoca, Risoprint Publishing house, 2010.
[30] Florescu-Gligore, Adrian, Magdalena Orban and Ştefan Ţălu. *Cotarea în proiectarea constructivă şi tehnologică. (Dimensioning in technological and constructive engineering graphics).* Cluj-Napoca, Lithography of The Technical University of Cluj-Napoca, 1998.
[31] Florescu-Gligore, Adrian, Ştefan Ţălu and Dan Noveanu. *Reprezentarea şi vizualizarea formelor geometrice în desenul industrial. (Representation and visualization of geometric shapes in industrial drawing).* Cluj-Napoca, U. T. Pres Publishing house, 2006.
[32] Ţălu, Ştefan and Cristina Racocea. *Reprezentări axonometrice cu aplicaţii în tehnică. (Axonometric representations with applications in technique).* Cluj-Napoca, MEGA Publishing house, 2007.
[33] Racocea, Cristina and Ştefan Ţălu. *Reprezentarea formelor geometrice tehnice în axonometrie. (The axonometric representation of technical geometric shapes).* Cluj-Napoca, Napoca Star Publishing house, 2011.
[34] Niţulescu, Theodor and Ştefan Ţălu. *Aplicaţii ale geometriei descriptive şi graficii asistate de calculator în desenul industrial. (Applications of descriptive geometry and computer aided design in engineering graphics).* Cluj-Napoca, Risoprint Publishing house, 2001.
[35] Bîrleanu, Corina and Ştefan Ţălu. *Organe de maşini. Proiectare şi reprezentare grafică asistată de calculator. (Machine elements. Designing and computer assisted graphical representations).* Cluj-Napoca, Victor Melenti Publishing house, 2001.
[36] Ţălu, Ştefan. *Micro and nanoscale characterization of three dimensional surfaces. Basics and applications*. Napoca Star Publishing House, Cluj-Napoca, Romania, 2015.
[37] *** Certification tests of LPG and CNG. Accessed January 10, 2018. http://vzlutest.cz/en/certification-tests-of-lpg-and-cng-c3.html.
[38] Nash, H. David. "UK Rules for unfired pressure vessels". In: "The Companion guide to ASME boiler and pressure vessel code", 2008. ASME, Chapter 51. ISBN 9780971902717. Accessed January 10, 2018. https://strathprints.strath.ac.uk/6502.
[39] *** Autodesk AutoCAD 2017 software.
[40] *** SolidWorks 2017 software.